Dynamic life cycle assessment of energy technologies under different greenhouse gas concentration pathways

Kai Lan[1], Yuan Yao[1,*]

[1]Center for Industrial Ecology, Yale School of the Environment, Yale University,
380 Edwards Street, New Haven, Connecticut, 06511, United States
*Email: y.yao@yale.edu

Abstract

Global warming potential (GWP) has been widely used in the Life Cycle Assessment (LCA) to quantify the climate impacts of energy technologies. Most LCAs are static analyses without considering the dynamics of Greenhouse Gas (GHG) emissions and changes in background GHG concentrations. This study presents a dynamic approach to analyze the life-cycle GWP of energy technologies in different timeframes and representative GHG concentration pathways. Results show that higher atmospheric GHG concentrations lead to higher life-cycle GWP for long-term analysis. The impacts of background GHG concentrations are more significant for technologies with large operational emissions or CH_4 emissions than technologies with low operational emissions. The case study for the U.S. electricity sector in 2020–2050 shows the impacts of background GHG concentrations and different LCA methods on estimating national climate impacts of different energy technology scenarios. Based on the results, it is recommended for future LCAs to incorporate temporal effects of GHG emissions when (1) technology has large operational GHG emissions or CH_4 emissions; (2) the analysis timeframe is longer than 50 years; (3) when LCA results are used for policymaking or technology comparisons for mitigating climate change.

Keywords: life cycle assessment, dynamic modeling, carbon analysis, greenhouse gas emissions, power generation, global warming potential

Synopsis

This study developed a dynamic life cycle assessment approach to incorporate the temporal dynamics of atmospheric GHG concentrations and GHG emissions into Global Warming Potential accounting of energy technologies.

TOC/Abstract Art

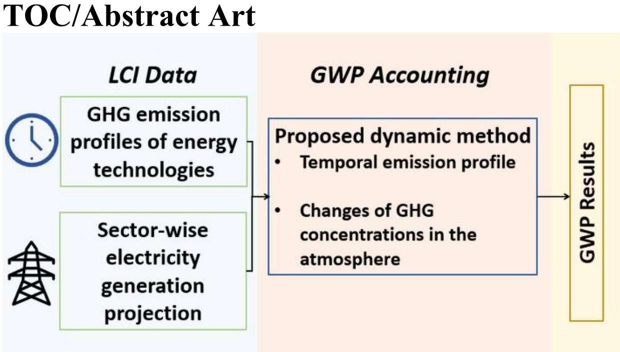

1. INTRODUCTION

The energy sector is one of the largest contributors to greenhouse gas (GHG) emissions in the world and accounts for 73% of total global GHG emissions in 2016.[1] To reduce GHG emissions, different climate change mitigation scenarios have been proposed by adopting emerging technologies such as carbon capture and sequestration (CCS) and renewable energy (e.g., solar and wind) for the energy sector.[2–7] Quantifying and comparing the climate change mitigation potentials of different technologies and adoption scenarios from a holistic, life-cycle perspective is critical for energy policymaking and technology development.[8] Such comparison is challenging given the dynamic nature of both climate and GHG emission profiles of energy technologies.[9,10] Global Warming Potential (GWP) is a standard metric widely used in Life Cycle Assessment (LCA) to compare the climate impacts of different technologies.[11,12] GWP is calculated by the integrated radiative forcing of an emitted GHG and the reference gas carbon dioxide (CO_2).[11,13] The radiative forcing of a GHG over a time horizon is given by multiplying radiative efficiency and GHG remaining in the atmosphere after the pulse emission (well known as the impulse response function (IRF)).[11,14] Most LCA studies are static analyses and they use fixed GWP conversion factors for non-CO_2 GHG emissions. Several studies proposed dynamic frameworks considering the temporal effects of GHG emissions and varied time horizons,[8,9,22–24,13,15–21] and a few of them applied the dynamic approaches to LCA.[9,13,15–17,23,24] Several studies also presented dynamic GWP characterization factors with considering the temporal effects of GHG emissions, most of which focused on biogenic carbon issues.[16,17,22,24] Other studies developed correction methods for the fixed GWP factors (e.g., GWP*) to consider the warming equivalent effects of short-lived climate pollutants (e.g., CH_4).[25–27] The detailed review is available in Supporting Information (SI) Section 1. However, few studies have included the temporal changes of future background atmospheric GHG concentrations that have significant impacts on GWP results given its large correlation with radiative efficiency, a key parameter used in the radiative forcing calculation.[18,28] Quantitative understandings of the life cycle GWP impact of diverse energy technologies are essential to determine and compare the net climate change mitigation potential of different technologies. The static LCA method excludes dynamic factors such as the future changes in the atmospheric GHG concentrations that impact the life cycle GWP results, limiting the understandings of prospective climate implications of different energy technologies. In the current context of decarbonization, considering the dynamics of GHG emissions, decay, and atmospheric concentration changes in GWP accounting contributes to a fuller picture in the policy-relevant analysis (e.g., analyzing GWP reduction target[9]), especially in the analysis with emission profiles over a long time (typically longer than 20 years).[13,18]

To address the challenge, we developed a dynamic method integrated with LCA that is capable of modeling temporal dynamics of background GHG concentrations in the atmosphere and GHG emissions associated with energy systems. The method was used to analyze the dynamic life-cycle GWP of energy technologies under different trajectories of atmospheric GHG concentrations. In this method, the radiative efficiency is dependent on atmospheric GHG concentrations by using Representative Concentration Pathway (i.e., RCP2.6, RCP4.5, RCP6, RCP8.5),[29] instead of being fixed values in traditional GWP estimations. To understand the impacts of varied future atmospheric GHG concentration pathways on life-cycle GWP of energy technologies, this dynamic method was applied to nine power generation technologies (e.g., coal, natural gas, wind) and then scaled up for the U.S. electricity generation projection from 2020 to 2050 under varied CCS technology adoption scenarios. The results of the dynamic method in this study are compared to two common approaches in current LCAs to exhibit the significance of considering the changes of background GHG concentrations and the temporal effects of GHG emissions.

2. MATERIALS AND METHODS

In this study, a dynamic GWP accounting method was developed to incorporate the dynamic profiles of atmospheric GHG concentrations and GHG emissions (Section 2.1).[29] This method allows for dynamic assessment of climate impact in LCA. The method was first used to analyze the life-cycle GWP of various energy technologies on the basis of 1 kWh of electricity generated (functional unit) using the Life Cycle Inventory (LCI) data collected from the literature (Section 2.2). The GWP results of energy technologies were then scaled up using the projection of U.S. electricity generation by different fuel types and technology adoption from 2020 to 2050 (Section 2.3), providing national-level insights on prospective climate implications of different energy technology scenarios. To better understand the importance of considering GHG concentration in GWP accounting, the method developed by this study was compared with another two common approaches under different adoption scenarios of CCS technology. One is the traditional LCA approach that considers no temporal impacts of GHG emissions and uses GWP conversion factors for different GHGs over a fixed time horizon (e.g., 20 or 100 years).[28] The other is the dynamic method used in previous LCAs that only considers the decay of GHG species with fixed radiative efficiency.[9,15–17] In this study, the modeling work of dynamic GWP accounting is performed in Excel with VBA programming.

2.1. Dynamic GWP Accounting Method.

According to the Intergovernmental Panel on Climate Change (IPCC) 2013 report,[11] the GWP for gas i can be derived by eq 1:

$$GWP_i(H) = \frac{AGWP_i(H)}{AGWP_{CO_2}(H)} = \frac{\int_0^H RF_i(t)dt}{\int_0^H RF_{CO_2}(t)dt} \quad (1)$$

where $AGWP_i(H)$ is the absolute global warming potential (AGWP) (W yr m^{-2} kg^{-1}) due to the 1 kg pulse emission of gas i in the time horizon H (year), RF_i is the radiative forcing (RF) due to pulse emission of gas i. RF_i can be given by:

$$RF_i = A_i C_i \quad (2)$$

where A_i is the RF_i per unit mass increase of species i (or so-called radiative efficiency (RE)), C_i is the fraction of species i remaining in the atmosphere after the pulse emission (or so-called impulse response function, IRF).[11] A_i depends on the atmosphere concentration of gas i that is time-dependent and have been predicted by different concentration pathways.[29]

As RF related data is usually reported on an annual basis (e.g., GHG atmospheric concentration), this study adapted the discrete accounting method developed by Levasseur et al.[9] This method uses dynamic characterization factor $DCF_i(k)_{inst}$, to quantify the RF occurring in 1 year after k years of 1 kg pulse emission for gas i by eq 3.[9,15]

$$DCF_i(k)_{inst} = \int_{k-1}^{k} A_i(k) C_i(t)dt \quad (3)$$

where $A_i(k)$ is the radiative efficiency at k years after the pulse emission. $A_i(k)$ is time-dependent and varies for different GHG atmospheric concentrations. $C_i(t)$ is the time-dependent C_i during year k. The cumulative DCF for gas i with a time horizon H will be equal to AGWP:

$$DCF_i(H)_{cumu} = \sum_{k=0}^{H} DCF_i(k)_{inst} = AGWP_i(H) \quad (4)$$

For GHG emitted in year j, $g_i(j)$ in kg, the instantaneous global warming impact in year k, $GWI_{inst}(k)$, can be derived from the instantaneous RF as shown in eq 5.[17]

$$GWI_{inst}(k) = \sum_i \sum_{j=0}^{k} g_i(j) \times DCF(k-j)_{inst} \quad (5)$$

The cumulative global warming impact for a time horizon H, $GWI_{inst}(H)$, can be calculated by summing up $GWI_{inst}(k)$ as shown in eq 6.[17]

$$GWI_{cumu}(H) = \sum_{k=0}^{H} GWI_{inst}(k) \quad (6)$$

The global warming potential of the GHG in the reference of CO_2, GWP (kgCO_2-eq), can be derived by eq 7.[15] $DCF_{CO_2}(H)_{cumu}$ is the cumulative DCF for 1 kg CO_2 pulse emission in year 0 and calculated from eq 4.

$$GWP = \frac{GWI_{cumu}(H)}{DCF_{CO_2}(H)_{cumu}} \quad (7)$$

Two important parameters in the calculations presented above are $A_i(k)$ and $C_i(t)$ that need be calculated for individual GHG.

For CO_2, the IRF (C_{CO_2}) is approximated by the summation of exponentials:[11,30]

$$C_{CO_2}(t) = a_0 + a_1 e^{(-\frac{t}{\tau_1})} + a_2 e^{(-\frac{t}{\tau_2})} + a_3 e^{(-\frac{t}{\tau_3})} \quad (8)$$

where τ is the lifetime of perturbation (year), a_0 = 0.2173, a_1 = 0.2240, a_2 = 0.2824, a_3 = 0.2763, τ_1 = 394.4 year, τ_2 = 36.54 year, τ_3 = 4.304 year. A_{CO_2} is approximated by using the derivative of CO_2 RF based on work by Myhre el at.[11,31]

$$A_{CO_2} = \frac{dRF_{CO_2}}{dC} = \frac{d}{dC}\left[\alpha \ln\left(\frac{C}{C_0}\right)\right] = \frac{\alpha}{C} \quad (9)$$

where C is the CO_2 concentration in the atmosphere (in ppm), C_0 is the reference concentration. In this study, $\alpha = 5.35$ W m^{-2} based on the IPCC report.[11] Hence, in year k, the $A_{CO_2}(k)$ is:

$$A_{CO_2}(k) = \frac{\alpha}{C(k)} \quad (10)$$

Using eq 3, the instantaneous DCF of CO_2 is:

$$DCF_{CO_2}(k)_{inst} = \int_{k-1}^{k} A_{CO_2}(k) C_{CO_2}(t) dt \quad (11)$$

For CH_4, the IRF (C_{CH_4}) is expressed as exponential decay by using CH_4 lifetime of perturbation τ_{CH_4} = 12.4 year.[11]

$$C_{CH_4}(t) = e^{\left(-\frac{t}{\tau_{CH_4}}\right)} \tag{12}$$

Similar to the calculations for CO_2, the A_{CH_4} is given by using the derivative of RF as shown in eq 13 and 14.[11,31]

$$A_{CH_4} = \frac{dRF_{CH_4}}{dM} = \frac{d}{dM}\left(\alpha\left(\sqrt{M} - \sqrt{M_0}\right) - \left(f(M, N_0) - f(M_0, N_0)\right)\right) = \frac{d}{dM}\left(\alpha\sqrt{M}\right) - \frac{d}{dM}\left(f(M, N_0)\right) \tag{13}$$

$$f(M, N) = 0.47 \ln\left(1 + 2.01 \times 10^{-5} \times (MN)^{0.75} + 5.31 \times 10^{-15} \times M \times (MN)^{1.52}\right) \tag{14}$$

where M is the CH_4 concentration in the atmosphere (in ppb), M_0 is the CH_4 reference concentration, N_0 is the N_2O reference concentration, α = 0.036 W m^{-2}.[11] Then the instantaneous DCF of CH_4 is given by:

$$DCF_{CH_4}(k)_{inst} = (1 + f_1 + f_2)\int_{k-1}^{k} A_{CH_4}(k)C_{CH_4}(t)dt \tag{15}$$

where f_1 = 0.5 reflecting the indirect effects on ozone, f_2 = 0.15 reflecting the indirect RF from CH_4 via changes in stratospheric H_2O.[11,32–36]

For N_2O, the IRF (C_{N_2O}) is expressed as exponential decay by using N_2O lifetime of perturbation τ_{N_2O} = 121 year.[11]

$$C_{N_2O}(t) = e^{\left(-\frac{t}{\tau_{N_2O}}\right)} \quad (16)$$

A_{N_2O} is given by using the derivative of RF as shown in eq 17 using the function *f(M,N)* in eq 14.[11,31]

$$A_{N_2O} = \frac{dRF_{N_2O}}{dM} = \frac{d}{dM}\Big(\alpha\big(\sqrt{N} - \sqrt{N_0}\big) - \big(f(M_0, N) - f(M_0, N_0)\big)\Big) = \frac{d}{dM}\big(\alpha\sqrt{N}\big) - \frac{d}{dM}\big(f(M_0, N)\big) \quad (17)$$

where N is the N_2O concentration in the atmosphere (in ppb), α = 0.12 W m^{-2}.[11] Then the instantaneous DCF of N_2O is given by:

$$DCF_{N_2O}(k)_{inst} = (1 - 0.36(1 + f_1 + f_2)\frac{A_{N_2O}(k)}{A_{CH_4}(k)})\int_{k-1}^{k} A_{N_2O}(k)C_{N_2O}(t)dt \quad (18)$$

where f_1 and f_2 are the same as that in eq 15.

In this study, the GHG atmospheric concentrations in four widely recognized prediction pathways (RCP2.6, RCP4.5, RCP6, RCP8.5) were used to assign the projected values for C (CO_2 concentration in the atmosphere), M (CH_4 concentration in the atmosphere), and N (N_2O concentration in the atmosphere).[29]

2.2. GHG Emission Profiles of Energy Technologies.

In this study, nine types of power generation technologies are included: coal and natural gas (NG) with and without CCS, nuclear, hydropower, geothermal, photovoltaic (PV), and wind. The energy technologies that account for less than 0.5% of total U.S. electricity generation from 2020 to 2050 were excluded.[2] The U.S. electricity generation from 2020 to 2050 follows the reference case projection of the U.S. Energy Information Administration (EIA) Annual Energy Outlook (AEO) 2019 (see Section 2.3 for details).[2] For each power generation technology, two life-cycle stages were included for the LCI data: upstream stage in year 0 (i.e., raw materials extraction and production, transportation, and on-site construction) and operational stage (i.e., fuel combustion, plant operations and maintenance) (see Figure S1 in SI for the system boundary).[37,38] Based on the LCI data of various power generation technologies harmonized by the U.S. National Renewable Energy Laboratory (U.S. NREL),[37] the life span of energy technologies was selected to be 30-year that was frequently used in the literature.[37–43] The cradle-to-gate LCI data of GHG emissions (i.e. CO_2, CH_4, and N_2O) for different electricity generation technologies (including coal and NG with CCS) were collected from the literature based on 1 kWh (functional unit) of net electricity generation (see SI Table S2 for detailed data).[2,37–45] As this study focuses on developing a dynamic GWP accounting framework for LCA, the effects of future technological development, policies, and market conditions on these LCI data are not included. However, the LCI data can be updated and tailored by future researchers upon their needs and data availability.

2.3 Scenario Analysis for Prospective Life-cycle GWP of U.S. Electricity Generation

To understand the policy/practical implications of our method, we applied it to a case study of U.S. electricity generation from 2020–2050 with different technology adoption scenarios. The annual projections of total U.S. electricity generation from 2020 to 2050 by different generation technologies followed the reference case projection of the AEO 2019.[2] This projection represented EIA's assessment of how the U.S. power sector would operate through 2050 under current laws and regulations, which could be interpreted as a baseline case.[2] It is noticeable that the power sector projections are subjected to many uncertainties (e.g., technology development, demographics, policies, regulations).[2] Hence, the 2020–2050 projection data used in this case study can be further modified by researchers for future research upon different assumptions and data availability. Other projection cases from the AEO (e.g., high or low economic growth case) and Electrification Futures Study by U.S. NREL are also valuable data sources for future studies in this area.[2,46]

It is expected that the adoption of CCS and renewable energy will mitigate the climate impacts of the U.S. electricity generation. CCS represents a group of promising technologies that capture and store CO_2 and in underground carbon reservoirs (e.g., saline aquifers, depleted oil and gas formations).[47–50] The questions are when and how fast those technologies should be adopted to achieve specific climate change mitigation goals from a life-cycle perspective. As the answers are time-dependent, considering the dynamics of both GHG emissions and background GHG concentration in the atmosphere is necessary.

In this study, five scenarios of the CCS adoption in the electricity generation projection were investigated, including a business-as-usual (BAU) scenario, three scenarios for adopting CCS at low, medium, and high adoption rate respectively, and one scenario for the late adoption of CCS.[51–55] The adoption of CCS in the case study was modeled by applying an adoption ratio to net electricity generation (kWh) of coal or NG power plants. The adoption ratio in each scenario was assumed based on the literature data that previously investigated the projections of CCS adoption (see Table S1 for CCS adoption ratio).[51–55] Using the LCI data of different electricity generation technologies, the total 2020-2050 emission profile can be derived as shown in eq 19. *E(i,j)* represents the annual emission of GHG *i* (*i* includes CO_2, CH_4, N_2O); *LCI(n,i)* (g/kWh) is the quantity of GHG *i* for technology *n* (documented in SI Table S2); *P(n,j)* is the projections of technology *n* in year *j* (see SI Tables S3–S7). The projections of coal and natural gas power generation with CCS were estimated using the adoption ratio mentioned above. The detailed models were documented in SI Section 2.

$$E(i,j) = \sum_{n=1}^{9} LCI(n,i)P(n,j) \quad (19)$$

The baseline BAU (business-as-usual) assumes that the future electricity production mix will be the same as that in 2020 (see SI Table S3). The late adoption case assumed that the adoption of CCS would be as late as 2035, but the adoption rate was high enough to catch up with the previous high adoption scenario. This scenario was designed to understand the impacts of adoption time (see SI Table S7). The adoption of renewable energy was kept to be the same with the projection in 2050 developed by the U.S. EIA.[2] The assumptions of each scenario are summarized in Table 1.

In each scenario, three GWP accounting methods were used to quantify the GWP of annual U.S. electricity generation, namely the static practice in LCA (i.e., the traditional LCA approach), dynamic LCA with fixed GHG concentrations, and dynamic GWP accounting method in this study with varied GHG atmospheric concentration pathways (i.e., RCP2.6, RCP4.5, RCP6, RCP8.5). This study does not intend to project and reconcile the global GHG concentration pathways under varied U.S. power sector scenarios. Instead, we quantify the impacts of varied GWP accounting methods and concentration pathways on the GWP results of the U.S. power sector. In other words, the scenario analysis attempts to answer the "what-if" question, namely how the GWP results of the U.S. power generation would change if the GHG concentrations follow different pathways. Hence, this study does not consider the interdependency of future U.S. power sector scenarios and global GHG concentration pathways. However, this can be explored in future research upon available data or using global integrated assessment models.

Table 1. Assumptions of Five Scenarios for U.S. Electricity Generation from 2020 to 2050

Scenario	Assumptions	GWP accounting methods
Business-as-usual (BAU)	The future electricity production mix will be the same as that in 2020 (SI Table S3). The total electricity production is based on EIA reference case projection.	1) Static practice in LCA; 2) dynamic LCA with fixed GHG concentrations; 3) dynamic LCA with varied GHG atmospheric concentration projections (i.e. RCP2.6, RCP4.5, RCP6, RCP8.5).
Low adoption	EIA reference case projection with low CCS adoption rate (22% by 2050 with linear growth) from 2020-2050 (SI Table S4).	
Medium adoption	EIA reference case projection with medium CCS adoption rate (30% by 2050 with linear growth) from 2020-2050 (SI Table S5).	
High adoption	EIA reference case projection with high CCS adoption rate (86% by 2050 with linear growth) from 2020-2050 (SI Table S6).	
Late adoption	The adoption of CCS would start as late as 2035, but the adoption rate (86% by 2050 with linear growth) would be high to catch up with the high adoption scenario in year 2050 (SI Table S7).	

3. RESULTS AND DISCUSSION

3.1. GWP of 1 kg of Pulse Emission in Year 0.

Figure 1 shows the GWP characterization factors calculated for 1kg of pulse emission CH_4 (Figure 1a) and dinitrogen monoxide N_2O (Figure 1b) in year 0 using the dynamic method developed in this study compared with the traditional static approach and dynamic LCA that uses fixed GHG concentration. The GWP results of 1 kg of pulse emission CO_2, CH_4, and N_2O in other years (i.e., year 10, 25, 50, and 75) are available in Table S8 in SI. GWP factors are shown from 20 to 100 years to be consistent with the time horizons showed by IPCC.[28] The GWP characterization factors for fixed 20- and 100-year timeframe from IPCC are shown as black crosses in year 20 and 100, which are the factors used in traditional static LCA. The dynamic method developed by previous studies can provide time-dependent GWP, but their factors are based on fixed atmospheric GHG concentrations (orange lines). The dynamic GWP factors developed using our method were presented under four RCPs.[29] Figure 1a indicates that both static and dynamic LCA with fixed GHG concentrations underestimate the GWP of CH_4 (e.g., 14.9%–29.4% lower than our method at 100-year time horizon), although different dynamic methods showed similar trends as time horizon increases. Among the results of our method, RCP with higher GHG concentrations shows lower CH_4 GWP factors when the time horizon is shorter than 53-year. However, this trend reverses after a 53-year time horizon, as shown in Figure 1a. For N_2O, only the results of RCP2.6 and RCP4.5 show similar trends with the results of dynamic method with fixed GHG concentrations, while the results of RCP6 and RCP8.5 show significant increases with the longer time horizon. Compared to the 100-year result of static LCA, the GWP factor of N_2O in varied RCP are 5.9%–45.9% larger. These large discrepancies among different methods for CH_4 and N_2O indicate the necessity of including temporal impacts and background atmospheric GHG concentrations in LCA or relevant carbon analysis, especially for those power generation technologies with significant life-cycle CH_4 and N_2O emissions.

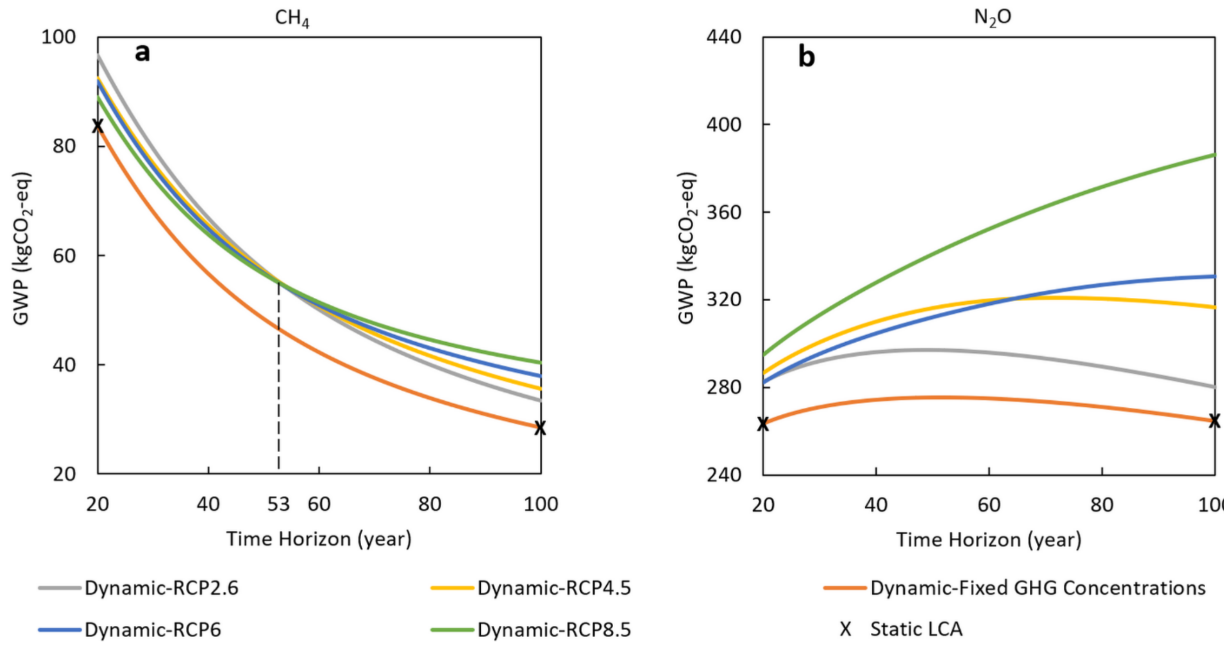

Figure 1. GWP factors of 1 kg of pulse emission in year 0 with different time horizons: (a) CH_4; (b) N_2O.

3.2. GWP of Energy Technologies Under Different GHG Concentration Pathways.

Figure 2 shows the dynamic life-cycle GWP of nine energy technologies under different RCP compared with the results using traditional methods. The results of four time horizons (35, 50, 75, and 100 years) are presented, since the time horizon needs to be longer than the operational stage of the LCI data (30 years) for varied generation technologies. The results of nine energy technologies are categorized into three groups based on their GHG emission profiles, including (1) CO_2-emission-dominated systems with large operational emissions annually (i.e., coal, NG, and nuclear that have higher life-cycle CO_2 emissions compared to the CH_4 and N_2O emissions of the same technology; they also have higher operational emissions than their upstream emissions); (2) CH_4-emission-dominated systems (i.e., the GWP results of coal and NG with CCS are largely driven by CH_4 emissions (see SI Table S1)); (3) CO_2-emission-dominated systems with large embedded emissions but small operational emissions (i.e., hydropower, geothermal, PV, and wind).

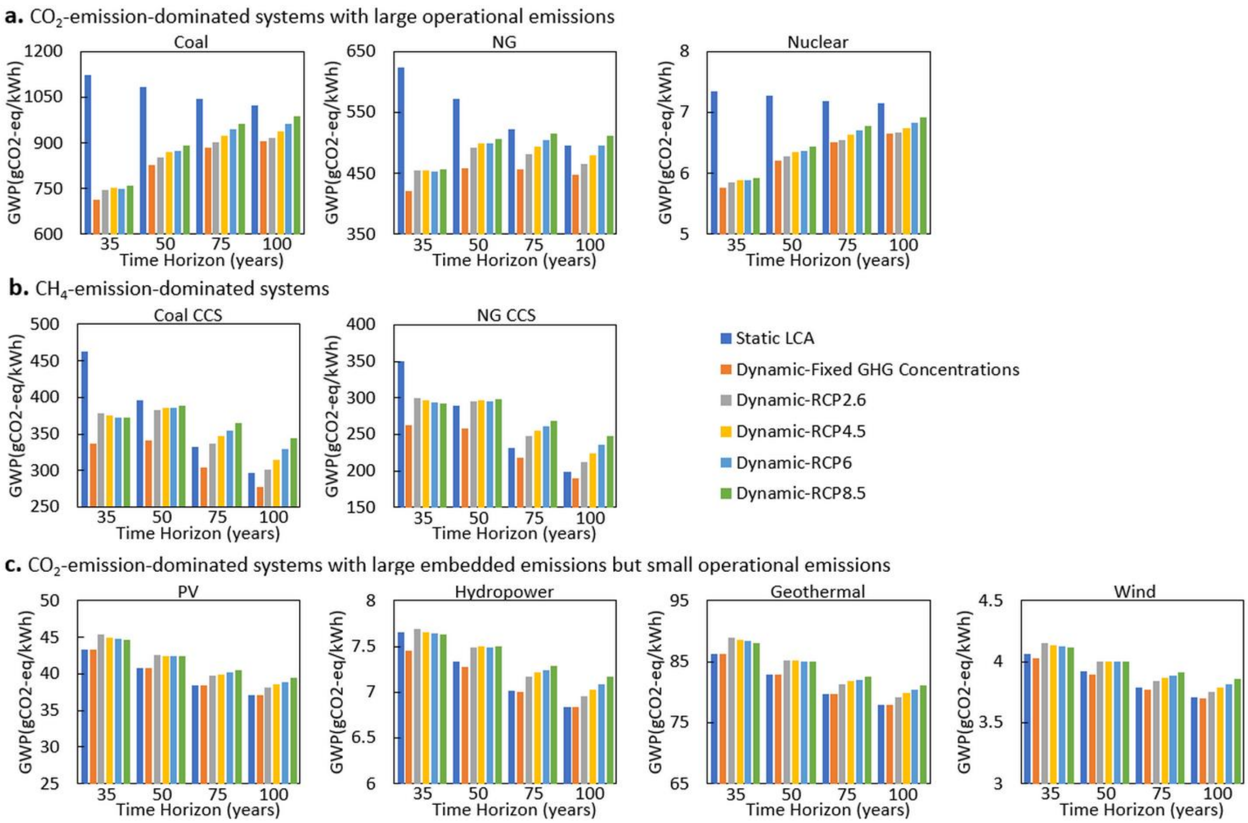

Figure 2. Life-cycle GWP of energy technology (functional unit: 1 kWh) under different RCP using our method compared with the results of traditional static and dynamic LCA approaches: (a) CO_2-emission-dominated systems with large operational emissions; (b) CH_4-emission-dominated systems; (c) CO_2-emission-dominated systems with large embedded emissions but small operational emissions.

Figure 2 indicates significant differences in the GWP results between static and dynamic LCAs, and such differences varied by time horizons and technology groups (percentage difference results are presented in Figure S2). For nine technologies, static LCA shows decreased GWP with longer time horizons due to lower GWP characterization factors for non-CO_2 gases in the longer-term (e.g., the GWP characterization factor for CH_4 is 62 for 35 years, 58 for 50 years, and 28 for 100 years, see Figure 1) . However, for a specific time horizon, the current static LCA is unable to keep a consistent timeframe for GHG emissions occurring in different years. For example, a static LCA choosing 100-year fixed GWP characterization factors consider the impacts of all emissions for 100 years. Thus, the GWP of emission in year 50 includes the impact from year 50 to year 150;

while the GWP of emission in year 75 includes the impact from year 75 to year 175. For an analysis with a fixed time horizon (e.g., a climate policy analysis for the future 100 years), this static approach includes the impacts beyond the scope of 100 years and does not distinguish earlier and later emissions. Oppositely, the dynamic LCA method has a consistent time horizon for all GHG emissions in the same analysis, as the GWP impacts beyond the chosen time horizon *H* are excluded (see eq 1). For example, if the time horizon is set to 100 years, the impacts of emission in year 50 are only considered for the remaining 50 years. This approach also distinguishes the impacts of earlier and later emissions. Therefore, dynamic LCAs for operational-CO_2-intensive technologies (i.e., coal, NG, and nuclear) in Figure 2a showed lower GWP than static LCA, while the differences between static and dynamic LCAs are reduced with the longer time horizon as the GHG decay is closer to stagnation (reflected by impulse response function with longer time horizons[28]). For later emissions, their relative contributions compared to earlier emissions increase as the time horizon increases, which explains why all dynamic LCAs in coal and nuclear have higher GWP with longer time horizons. For example, in Figure 2a, when expanding the time horizon from 35 years to 100 years, the GWP of coal-based electricity generation increases 23.3%–30.2% across varied RCP. Figure 2a shows that RCP cases have higher GWP results than the results of dynamic LCA with fixed GHG concentrations. The higher GHG concentration, the larger differences between the RCP case and fixed GHG concentration case. For example, for coal in Figure 2a, RCP2.6 exhibits 1.2%–4.2% higher GWP than dynamic LCA with fixed GHG concentrations, while RCP8.5 shows a 6.4%–9.1% difference. For NG in Figure 2a, expanding the time horizon fails to show significant increases in GWP and even shows slight decreases in some cases (e.g., RCP2.6 and RCP4.5). This can be explained that over coal and nuclear, NG has more GHG emissions coming from CH_4 (see SI Table S1) and gains the combined effects from the first group (CO_2-emission-dominated systems with large operational emissions in Figure 2a) and the second group (CH_4-emission-dominated technologies).

For CH_4-emission-dominated technologies, atmospheric GHG concentrations have large impacts on the GWP in the long term, and such impacts are overlooked by static LCA and dynamic LCA with fixed GHG concentrations. Different from Figure 2a where dynamic LCAs in coal and nuclear have higher GWP with longer time horizons, GWP in Figure 2b by all dynamic methods has minor changes between 35 years and 50 years, and decreases when the time horizon changes from 50 years to 100 years, which is impacted by the trend of CH_4 (similar to Figure 1a). In Figure 2b, the differences among the four RCPs are much larger at a 100-year time horizon than 35-year, reflecting the increased impacts of both GHG decay and background GHG concentrations on the long-term projection. In Figure 2b, at the 100-year time horizon, both current static LCA and dynamic LCA with fixed GHG concentrations underestimate the GWP, given that both methods rely on the present-day GHG concentrations. For example, for NG with CCS, at the 100-year time horizon, results of RCPs are 6.8%–24.4% higher than current static LCA and 14.6%–30.1% higher than dynamic LCA with fixed GHG concentrations. The higher atmospheric GHG concentrations (e.g., RCP8.5), the larger the discrepancy is. For a shorter time horizon (e.g., 35 or 50 years), the GWP results of static LCA are close to (although slightly higher than) the results of our method. However, the GWP results of dynamic method with fixed GHG concentrations are much lower than our method's results because the former only accounts GHG emitting timeline without considering the changing radiative efficiency caused by the changing atmospheric GHG concentrations.

For CO_2-emission-dominated technologies with large embedded emissions but small operational emissions (i.e., PV, hydropower, geothermal, and wind in Figure 2c), the results of static LCA and dynamic LCA with fixed GHG concentrations are slightly lower than our method (e.g., 2.5%–6.1% lower than our method at 100-year time horizon for PV). Compared to the first (Figure 2a) and second (Figure 2b) groups of energy technologies, this group shows the smallest discrepancies of the results using static and dynamic approaches.

3.3. Meeting GHG Mitigation Targets Under Different GHG Concentration Pathways.

Figure 3 shows the total accumulative GWP reduction potential from 2020 to 2050 in four climate mitigation scenarios of projected electricity generation compared with BAU using the static LCA, dynamic LCA with fixed GHG concentrations, and our method with four RCP projections, with a 50-year time horizon. The year-by-year GWP reduction potentials are shown in Figure 4. The results of dynamic LCA with RCP6 are presented as an example. The results of four scenarios with 100-year time horizon are available in SI Figures S3 and S4.

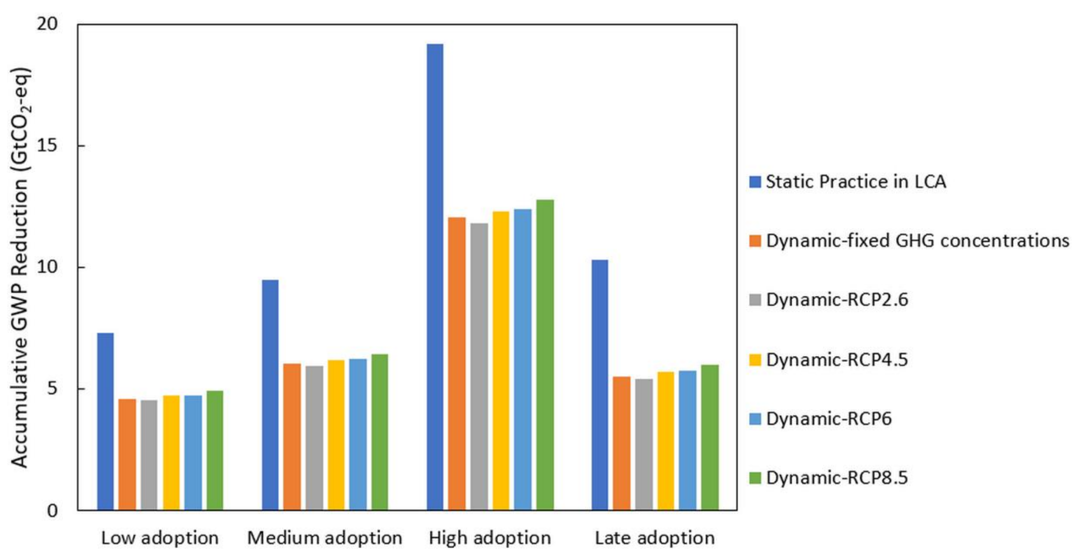

Figure 3. GWP (50-year time horizon) reduction potential by 2050 of four climate change mitigation scenarios compared with the BAU.

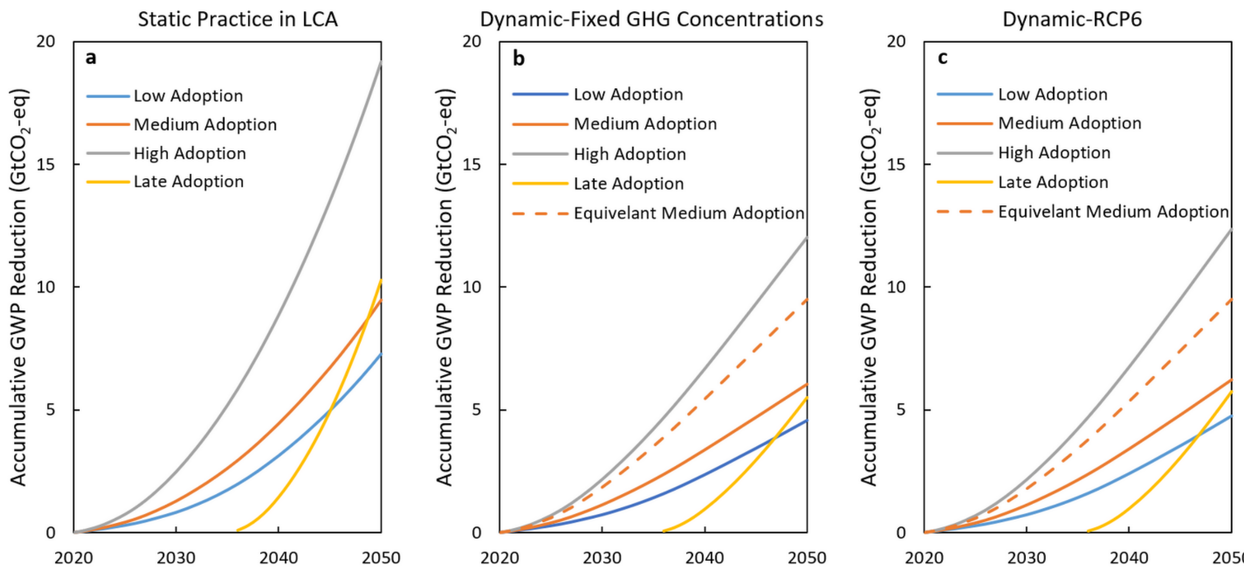

Figure 4. GWP (50-year time horizon) reduction potential of four climate change mitigation scenarios compared with the BAU: (a) static practice in LCA; (b) dynamic LCA with fixed GHG concentrations; (c) dynamic LCA with RCP6 projection.

Static LCA significantly overestimates the GWP mitigation potential of four scenarios (47.3%–90.3% higher as shown in Figure 3) compared to the results of dynamic LCA with fixed GHG concentrations and our dynamic approach. For example, in Figure 4, in the medium adoption scenario (orange solid line in Figure 4a), the GWP mitigation potential by 2050 is 9.5 $GtCO_2$-eq using static LCA, while that for the same scenario is 6.0 $GtCO_2$-eq for the dynamic method with fixed GHG concentrations and 6.2 $GtCO_2$-eq for the dynamic method with RCP6 projection. To reach the same GWP mitigation goal (9.5 $GtCO_2$-eq by 2050), the adoption rate of CCS needs to be as high as 57.6% by 2050 using the current dynamic GWP accounting method (plotted as the orange dashed line in Figure 4b) and 55.5% by 2050 using dynamic LCA with RCP6 (orange dash line in Figure 4c). Such adoption rate is 92% and 85% higher than the current medium adoption scenario, respectively.

The GWP mitigation potential of our dynamic LCA method shows differences from the current dynamic LCA. In Figure 3, compared with the results of dynamic LCA with fixed GHG concentrations, the accumulative GWP reduction estimated by our dynamic LCA methods are 1.2%–2.0% smaller in RCP2.6, 1.9%–3.7% larger in RCP4.5, 2.7%–4.5% larger in RCP6, and 6.2%–9.2% larger in RCP8.5. This is caused by the differences in the atmospheric GHG concentrations. As the RCP2.6 projection has the slightest difference with current atmospheric GHG concentrations, the RCP2.6 results have the smallest discrepancy with the current dynamic LCA that uses fixed atmospheric GHG concentrations.

For different RCP, the GWP reduction potential increases as RCP concentration increases, as shown in Figure 3. For example, in the medium adoption scenario, compared to RCP2.6 results, RCP4.5, RCP6, and RCP8.5 shows an increase of 3.8%, 4.6%, and 8.0%, respectively. This finding is critical for decision making that uses LCA results to support energy policy (e.g., setting mitigation goals) and technology investments (e.g., determining funding needs to accelerate the adoption of specific technologies), especially when the future atmospheric GHG concentration is different from current values.

Another observation is that the late adoption of CCS in the electricity sector with a high adoption rate will take a longer time to catch up with early adoption scenarios (low and medium adoption scenarios) in Figure 4c than Figure 4a, which leads to different comparative conclusions when investigating different scenarios in the same year. For example, in 2050, static LCA results indicate that the late adoption scenario leads to 8.7% more GWP reduction than the medium adoption scenario. This is too optimistic compared with dynamic LCA with RCP6 where the late adoption shows 7.8% less GWP reduction than the medium adoption. As the static LCA method does not differentiate earlier and later GHG emissions, the possible negative consequences of late adoption (e.g., reducing GWP reduction) are underestimated or overlooked. Hence, when using dynamic LCA methods, earlier adoption is more likely to reach a similar GWP mitigation goal with the static LCA method, and the differences between the two methods are impacted by different GHG concentrations in the atmosphere.

3.4. Limitations and Implications of Methods.

This study aims to provide a fuller picture of accounting life-cycle GWP in LCA by incorporating the dynamics in the atmospheric GHG concentrations and GHG emissions, demonstrated by a case study of the electricity generation sector in the U.S. The static method applies the same GWP characterization for GHG emitted at different years, ignoring the impacts of later and earlier emissions. The dynamic LCA approach in this study addresses this limitation by developing dynamic GWP characterization factors, considering the temporal profile of GHG emissions, and using a consistent time horizon for GWP accounting. Compared to the current dynamic LCA that uses fixed, present GHG concentrations, our method considers the future changes of the atmospheric GHG concentrations. The current dynamic LCA shows significant discrepancies in the GWP results for high RCP cases (compared to our method) when the GHG concentrations are much higher than the present. Compared to other methods such as GWP* (see SI Section 1 for literature review details), our method does not rely on correcting fixed GWP characterization factors by empirical parameters that are subjected to scenario assumptions and data. Instead, GHG concentration is directly incorporated into the GWP calculation to derive dynamic GWP characterization factors. Our dynamic approach also allows for a consistent time horizon for GWP assessment of GHGs emitted at different years, which is particularly useful for LCA applications in terms of keeping a coherent temporal system boundary.

As this study focuses on the U.S. only, it does not include the feedback loop between RCPs and GHG emissions that may need to be considered for global studies. Such feedback loop can be added by modeling the radiative efficiency of GHG as a function of both time and emissions $g_i(j)$ in eq 5. Such a function will need to be developed based on the dynamic and quantitative relationship between global emissions and atmospheric GHG concentration changes. Another research direction is integrating the impacts of prospective energy transformation pathways into the LCI data that commonly do not consider future changes.[57,58,59] One approach is leveraging prospective scenarios from integrated assessment models (IAMs) (e.g., IMAGE[60]) to simulate the LCI data of future energy technologies.[57,61] For future applications, by considering the temporal profile of emissions and the impacts of atmospheric GHG concentration changes on radiative efficiency, the method presented in this study can be integrated into other climate change related indicators, e.g., monetary values of GHG emissions,[62] social cost of GHG emissions,[63] and Global Temperature change Potential (GTP)[11].

The results of this study demonstrate the importance of incorporating atmospheric GHG concentrations into the life-cycle carbon accounting of energy technologies, especially under the following circumstances:

- When the technology has large operational GHG emissions or CH_4 emissions. Our results show that atmospheric GHG concentrations have significant impacts on the life-cycle GWP of CO_2-emission-dominated energy technologies with large operational emissions such as coal, natural gas, and nuclear, as well as CH_4-emission-dominated systems such as coal and natural gas with CCS. For those technologies, the static practice in LCA shows remarkable discrepancies in the GWP results compared with dynamic methods. Such discrepancies are minimal for CO_2-emission-dominated technologies with large embedded emissions but small operational emissions (i.e., hydropower, geothermal, PV, and wind), in which most of the emissions are released at the beginning.

- When the analysis timeframe is longer than 50 years and the GHG concentration in the atmosphere is likely to be different from the present concentration. Compared with our method, the dynamic LCA method using fixed present GHG concentrations underestimated the GWP of all technologies, such underestimation is more significant under high GHG concentration pathways such as RCP6 and RCP8.5. For the long-term time horizon (larger than 50 years), higher atmospheric GHG concentrations result in higher life-cycle GWP. Such trends are less significant for short-term analysis (50 years).
- When LCA results will be used to support policymaking or technology development for climate change mitigation in the future. The results of the case study for the U.S. electricity generation sector and different climate mitigation scenarios showed a large discrepancy of GWP mitigation potentials between our method and the static LCA approach that does not distinguish the impacts of early and later emissions. Our results indicate the necessity of earlier adoption of CCS to achieve the same climate change mitigation goals that use static LCA. These findings demonstrate the importance of considering the dynamics of background GHG concentrations in LCA and relevant environmental, policy, and technology decision making.

SUPPORTING INFORMATION

Literature review, detailed explanation of CCS adoption rate, LCI data of energy technologies, additional results, list of abbreviations and nomenclature, and references.

ACKNOWLEDGEMENTS

The authors thank the funding support from the U.S. National Science Foundation. This material is based upon work supported by the National Science Foundation under Grant No. 2038439. Any opinions, findings, and conclusions or recommendations expressed in this material are those of the author(s) and do not necessarily reflect the views of the National Science Foundation.

AUTHOR INFORMATION

Corresponding Author

Yuan Yao

Center for Industrial Ecology, Yale School of the Environment, Yale University, New Haven, Connecticut, 06511, United States;

E-mail: y.yao@yale.edu

Author

Kai Lan

Center for Industrial Ecology, Yale School of the Environment, Yale University, New Haven, Connecticut, 06511, United States.

REFERENCES

(1) World Resources Institute. World Greenhouse Gas Emissions: 2016 https://www.wri.org/data/world-greenhouse-gas-emissions-2016 (accessed June 12, 2021).

(2) U.S. EIA. *Annual Energy Outlook 2019 with Projections to 2050*; 2019. https://www.eia.gov/outlooks/aeo/pdf/aeo2019.pdf (accessed Apr 11, 2020).

(3) Buonocore, J. J.; Choma, E.; Villavicencio, A. H.; Spengler, J. D.; Koehler, D. A.; Evans, J. S.; Lelieveld, J.; Klop, P.; Sanchez-Pina, R. Metrics for the Sustainable Development Goals: Renewable Energy and Transportation. *Palgrave Communications* **2019**, *5*, 136.

(4) Cormos, C. C. Integrated Assessment of IGCC Power Generation Technology with Carbon Capture and Storage (CCS). *Energy* **2012**, *42*, 434–445.

(5) Blanco, T.; Rivas, C.; Ferna, J.; Artal, M.; Velasco, I. Influence of Methane in CO_2 Transport and Storage for CCS Technology. *Environmental science & technology* **2012**, *46*, 13016−13023.

(6) Blanco, T.; Rivas, C.; Fernández, J.; Artal, M.; Velasco, I. Discussion of the Influence of CO and CH4 in CO2 Transport , Injection, and Storage for CCS Technology. *Environmental science & technology* **2014**, *48*, 10984−10992.

(7) Maddali, V.; Tularam, G. A.; Glynn, P. Economic and Time-Sensitive Issues Surrounding CCS : A Policy Analysis. *Environmental science & technology* **2015**, *49*, 8959−8968.

(8) Sathre, R.; Masanet, E. Long-Term Energy and Climate Implications of Carbon Capture and Storage Deployment Strategies in the US Coal-Fired Electricity Fleet. *Environmental science & technology* **2012**, *46*, 9768–9776.

(9) Levasseur, A.; Lesage, P.; Margni, M.; Deschěnes, L.; Samson, R. Considering Time in LCA: Dynamic LCA and Its Application to Global Warming Impact Assessments. *Environmental science & technology* **2010**, *44* (8), 3169–3174.

(10) Pehl, M.; Arvesen, A.; Humpenöder, F.; Popp, A.; Hertwich, E. G.; Luderer, G. Understanding Future Emissions from Low-Carbon Power Systems by Integration of Life-Cycle Assessment and Integrated Energy Modelling. *Nature Energy* **2017**, *2*, 939-945.

(11) Myhre, G.; Shindell, D.; Bréon, F.-M.; Collins, W.; Fuglestvedt, J.; Huang, J.; Koch, D.; Lamarque, J. F.; Lee, D.; Mendoza, B.; Nakajima, T.; Robock, A.; Stephens, G.; Takemura T.; Zhang, H. Anthropogenic and Natural Radiative Forcing. In *Climate Change 2013: The Physical Science Basis. Contribution of Working Group I to the Fifth Assessment Report of the Intergovernmental Panel on Climate Change*; Stocker, T. F., Qin, D., Plattner, G.-K., Tignor, M., Allen, S. K., Boschung, J., Nauels, A., Xia, Y., Bex, V., Midgley, P. M., Eds.; Cambridge University Press: Cambridge, United Kingdom and New York, NY, USA, 2013.

(12) Jones, C.; Gilbert, P.; Stamford, L. Assessing the Climate Change Mitigation Potential of Stationary Energy Storage for Electricity Grid Services. *Environmental science & technology* **2020**, *54*, 67–75.

(13) Kendall, A.; Chang, B.; Sharpe, B. Accounting for Time-Dependent Effects in Biofuel Life Cycle Greenhouse Gas Emissions Calculations. *Environmental science & technology* **2009**, *43* (18), 7142–7147.

(14) Staples, M. D.; Malina, R.; Barrett, S. R. The Limits of Bioenergy for Mitigating Global Life-Cycle Greenhouse Gas Emissions from Fossil Fuels. *Nature Energy* **2017**, *2* (2), 1–8.

(15) Daystar, J.; Venditti, R.; Kelley, S. S. Dynamic Greenhouse Gas Accounting for Cellulosic Biofuels: Implications of Time Based Methodology Decisions. *International Journal of Life Cycle Assessment* **2017**, *22* (5), 812–826.

(16) Pingoud, K.; Ekholm, T.; Savolainen, I. Global Warming Potential Factors and Warming Payback Time as Climate Indicators of Forest Biomass Use. *Mitigation and Adaptation Strategies for Global Change* **2012**, *17* (4), 369–386.

(17) Han, J.; Canter, C.; Cai, H.; Wang, M.; Qin, Z.; Dunn, J. *Carbon Dynamics for Biofuels Produced from Woody Feedstocks*; Argonne, IL USA, 2018.

(18) Bright, R. M.; Cherubini, F.; Strømman, A. H. Climate Impacts of Bioenergy: Inclusion of Carbon Cycle and Albedo Dynamics in Life Cycle Impact Assessment. *Environmental Impact Assessment Review* **2012**, *37*, 2–11.

(19) Levasseur, A.; Lesage, P.; Margni, M.; Samson, R. Biogenic Carbon and Temporary Storage Addressed with Dynamic Life Cycle Assessment. *Journal of Industrial Ecology* **2013**, *17* (1), 117–128.

(20) Levasseur, A.; Lesage, P.; Margni, M.; Brandão, M.; Samson, R. Assessing Temporary Carbon Sequestration and Storage Projects through Land Use, Land-Use Change and Forestry: Comparison of Dynamic Life Cycle Assessment with Ton-Year Approaches. *Climatic Change* **2012**, *115* (3–4), 759–776.

(21) Edwards, M. R.; Trancik, J. E. Climate Impacts of Energy Technologies Depend on Emissions Timing. *Nature Climate Change* **2014**, *4* (5), 347–352.

(22) Faraca, G.; Tonini, D.; Astrup, T. F. Dynamic Accounting of Greenhouse Gas Emissions from Cascading Utilisation of Wood Waste. *Science of the Total Environment* **2019**, *651*, 2689–2700.

(23) Cherubini, F.; Peters, G. P.; Berntsen, T.; Strømman, A. H.; Hertwich, E. CO_2 Emissions from Biomass Combustion for Bioenergy: Atmospheric Decay and Contribution to Global Warming. *GCB Bioenergy* **2011**, *3*, 413–426.

(24) Dyckhoff, H.; Kasah, T. Time Horizon and Dominance in Dynamic Life Cycle Assessment. *Journal of Industrial Ecology* **2014**, *18* (6), 799–808.

(25) Lynch, J.; Cain, M.; Pierrehumbert, R.; Allen, M. Demonstrating GWP: A Means of Reporting Warming-Equivalent Emissions That Captures the Contrasting Impacts of Short- and Long-Lived Climate Pollutants. *Environmental Research Letters* **2020**, *15* (4), 044023.

(26) Cain, M.; Lynch, J.; Allen, M. R.; Fuglestvedt, J. S.; Frame, D. J.; Macey, A. H. Improved Calculation of Warming-Equivalent Emissions for Short-Lived Climate Pollutants. *npj Climate and Atmospheric Science* **2019**, *2* (1), 1–7.

(27) Allen, M. R.; Shine, K. P.; Fuglestvedt, J. S.; Millar, R. J.; Cain, M.; Frame, D. J.; Macey, A. H. A Solution to the Misrepresentations of CO2-Equivalent Emissions of Short-Lived Climate Pollutants under Ambitious Mitigation. *npj Climate and Atmospheric Science* **2018**, *1* (1), 1–8.

(28) IPCC. *Climate Change 2013: The Physical Science Basis. Contribution of Working Group I to the Fifth Assessment Report of the Intergovern- Mental Panel on Climate Change*; Stocker, T. F., Qin, D., Plattner, G.-K., Tignor, M., Allen, S. K., Boschung, J., Nauels, A., Xia, Y., Bex, V., Midgley, P. M., Eds.; Cambridge University Press: Cambridge, United Kingdom and New York, NY, USA, 2013.

(29) The International Institute for Applied Systems Analysis (IIASA). RCP Database (version 2.0) https://www.iiasa.ac.at/web-apps/tnt/RcpDb/dsd?Action=htmlpage&page=welcome#intro (accessed Aug 9, 2018).

(30) Joos, F.; Roth, R.; Fuglestvedt, J. S.; Peters, G. P.; Enting, I. G.; Von Bloh, W.; Brovkin, V.; Burke, E. J.; Eby, M.; Edwards, N. R.; Friedrich, T.; Frölicher, T. L.; Halloran, P. R.; Holden, P. B.; Jones, C.; Kleinen, T.; Mackenzie, F. T.; Matsumoto, K.; Meinshausen, M.; Plattner, G. K.; Reisinger, A.; Segschneider, J.; Shaffer, G.; Steinacher, M.; Strassmann, K.; Tanaka, K.; Timmermann, A.; Weaver, A. J. Carbon Dioxide and Climate Impulse Response Functions for the Computation of Greenhouse Gas Metrics: A Multi-Model Analysis. *Atmospheric Chemistry and Physics* **2013**, *13* (5), 2793–2825.

(31) Myhre, G.; Highwood, E. J.; Shine, K. P. New Estimates of Radiative Forcing Due to Well Mixed Greenhouse Gases. *Geophysical Research Letters* **1998**, *25* (14), 2715–2718.

(32) Shindell, D. T.; Faluvegi, G.; Bell, N.; Schmidt, G. A. An Emissions-Based View of Climate Forcing by Methane and Tropospheric Ozone. *Geophysical Research Letters* **2005**, *32* (4), 1–4.

(33) Shindell, D. T.; Faluvegi, G.; Koch, D. M.; Schmidt, G. a; Unger, N.; Bauer, S. E. Improved Attribution of Climate Forcing to Emissions. *Science* **2009**, *326* (5953), 716–718.

(34) Collins, W. J.; Fry, M. M.; Yu, H.; Fuglestvedt, J. S.; Shindell, D. T.; West, J. J. Global and Regional Temperature-Change Potentials for near-Term Climate Forcers. *Atmospheric Chemistry and Physics* **2013**, *13* (5), 2471–2485.

(35) Holmes, C. D.; Prather, M. J.; Søvde, O. A.; Myhre, G. Future Methane, Hydroxyl, and Their Uncertainties: Key Climate and Emission Parameters for Future Predictions. *Atmospheric Chemistry and Physics* **2013**, *13* (1), 285–302.

(36) Stevenson, D. S.; Young, P. J.; Naik, V.; Lamarque, J. F.; Shindell, D. T.; Voulgarakis, A.; Skeie, R. B.; Dalsoren, S. B.; Myhre, G.; Berntsen, T. K.; Folberth, G. A.; Rumbold, S. T.; Collins, W. J.; MacKenzie, I. A.; Doherty, R. M.; Zeng, G.; Van Noije, T. P.C.; Strunk, A.; Bergmann, D.; Cameron-Smith, P.; Plummer, D. A.; Strode, S. A.; Horowitz, L.; Lee, Y. H.; Szopa, S.; Sudo, K.; Nagashima, T.; Josse, B.; Cionni, I.; Righi, M.; Eyring, V.; Conley, A.; Bowman, K. W.; Wild, O.; Archibald, A. Tropospheric Ozone Changes, Radiative Forcing and Attribution to Emissions in the Atmospheric Chemistry and Climate Model Intercomparison Project (ACCMIP). *Atmospheric Chemistry and Physics* **2013**, *13* (6), 3063–3085.

(37) U.S. National Renewable Energy Laboratory. Life Cycle Assessment Harmonization https://www.nrel.gov/analysis/life-cycle-assessment.html (accessed Sep 9, 2019).

(38) Sproul, E.; Barlow, J.; Quinn, J. C. Time Value of Greenhouse Gas Emissions in Life Cycle Assessment and Techno-Economic Analysis. *Environmental science & technology* **2019**, *53* (10), 6073–6080.

(39) Whitaker, M.; Heath, G. A.; O'Donoughue, P.; Vorum, M. Life Cycle Greenhouse Gas Emissions of Coal-Fired Electricity Generation. *Journal of Industrial Ecology* **2012**, *16*, S53–S72.

(40) Hsu, D. D.; O'Donoughue, P.; Fthenakis, V.; Heath, G. A.; Kim, H. C.; Sawyer, P.; Choi, J. K.; Turney, D. E. Life Cycle Greenhouse Gas Emissions of Crystalline Silicon Photovoltaic Electricity Generation: Systematic Review and Harmonization. *Journal of Industrial Ecology* **2012**, *16*, S122–S135.

(41) Dolan, S. L.; Heath, G. A. Life Cycle Greenhouse Gas Emissions of Utility-Scale Wind Power: Systematic Review and Harmonization. *Journal of Industrial Ecology* **2012**, *16*, S136–S154.

(42) O'Donoughue, P. R.; Heath, G. A.; Dolan, S. L.; Vorum, M. Life Cycle Greenhouse Gas Emissions of Electricity Generated from Conventionally Produced Natural Gas: Systematic Review and Harmonization. *Journal of Industrial Ecology* **2014**, *18* (1), 125–144.

(43) Kim, H. C.; Fthenakis, V.; Choi, J.; Turney, D. E. Life Cycle Greenhouse Gas Emissions of Thin-Film Photovoltaic Electricity Generation. *Journal of Industrial Ecology* **2012**, *16*, S110–S121.

(44) Wernet, G.; Bauer, C.; Steubing, B.; Reinhard, J.; Moreno-Ruiz, E.; Weidema, B. The Ecoinvent Database Version 3 (Part I): Overview and Methodology. *International Journal of Life Cycle Assessment* **2016**, *21* (9), 1218–1230.

(45) Warner, E. S.; Heath, G. A. Life Cycle Greenhouse Gas Emissions of Nuclear Electricity Generation: Systematic Review and Harmonization. *Journal of Industrial Ecology* **2012**, *16*, S73–S92.

(46) Murphy, C.; Mai, T.; Sun, Y.; Jadun, P.; Muratori, M.; Nelson, B.; Jones, R. *Electrification Futures Study: Scenarios of Power System Evolution and Infrastructure Development for the United States;* Golden, CO, 2021.

(47) Wilson, E. J.; Friedmann, S. J.; Pollak, M. F. Research for Deployment: Incorporating Risk, Regulation, and Liability for Carbon Capture and Sequestration. *Environmental science & technology* **2007**, *41* (17), 5945–5952.

(48) Rubin, E. S.; Zhai, H. The Cost of Carbon Capture and Storage for Natural Gas Combined Cycle Power Plants. *Environmental science & technology* **2012**, *46*, 3076−3084.

(49) Stauffer, P. H.; Keating, G. N.; Middleton, R. S.; Viswanathan, H. S.; Berchtold, K. A.; Singh, R. P.; Pawar, R. J.; Mancino, A. Greening Coal: Breakthroughs and Challenges in Carbon Capture and Storage. *Environmental science & technology* **2011**, *45*, 8597–8604.

(50) Monroe, L. S.; Friedman, J. S. Deployment Models for Commercialized Carbon Capture And Storage. *Environmental science & technology* **2011**, *45* (1), 139–146.

(51) Clemmer, S.; Rogers, J.; Sattler, S.; Macknick, J.; Mai, T. Modeling Low-Carbon US Electricity Futures to Explore Impacts on National and Regional Water Use. *Environmental Research Letters* **2013**, *8* (1), 015004.

(52) Logan, J.; Lopez, A.; Mai, T.; Davidson, C.; Bazilian, M.; Arent, D. Natural Gas Scenarios in the U.S. Power Sector. *Energy Economics* **2013**, *40*, 183–195.

(53) Chandel, M. K.; Pratson, L. F.; Jackson, R. B. The Potential Impacts of Climate-Change Policy on Freshwater Use in Thermoelectric Power Generation. *Energy Policy* **2011**, *39* (10), 6234–6242.

(54) Katzer, J.; Moniz, E. J.; Deutch, J.; Ansolabehere, S.; Beer, J. *The Future of Coal: An Interdisciplinary MIT Study*; Cambridge, MA, 2007.

(55) Ross, M. T.; Fawcett, A. A.; Clapp, C. S. U.S. Climate Mitigation Pathways Post-2012: Transition Scenarios in ADAGE. *Energy Economics* **2009**, *31*, S212–S222.

(56) Arvesen, A.; Luderer, G.; Pehl, M.; Bodirsky, B.L.; Hertwich, E.G. Deriving life cycle assessment coefficients for application in integrated assessment modelling. *Environmental Modelling & Software* **2018**, *99*, 111-125.

(57) Arvesen, A.; Hertwich, E.G. Environmental implications of large-scale adoption of wind power: a scenario-based life cycle assessment. *Environmental Research Letters* **2011**, *6*(4), 045102.

(58) Pauliuk, S.; Arvesen, A.; Stadler, K. and Hertwich, E.G. Industrial ecology in integrated assessment models. *Nature Climate Change* **2017**, *7*(1), 13-20.

(59) Hertwich, E.G.; Gibon, T.; Bouman, E.A.; Arvesen, A.; Suh, S.; Heath, G.A.; Bergesen, J.D.; Ramirez, A.; Vega, M.I.; Shi, L. Integrated life-cycle assessment of electricity-supply scenarios confirms global environmental benefit of low-carbon technologies. *Proceedings of the National Academy of Sciences* **2015**, *112*(20), 6277-6282.

(60) Stehfest, E.; van Vuuren, D.; Bouwman, L.; Kram, T. *Integrated assessment of global environmental change with IMAGE 3.0: Model description and policy applications*; Netherlands Environmental Assessment Agency: The Hague, Netherlands.

(61) Mendoza Beltran, A., Cox, B., Mutel, C., van Vuuren, D.P., Font Vivanco, D., Deetman, S., Edelenbosch, O.Y., Guinée, J. and Tukker, A. When the background matters: using scenarios from integrated assessment models in prospective life cycle assessment. *Journal of Industrial Ecology*, **2020**, *24*(1), 64-79.

(62) Dong, Y.; Hauschild, M.; Sørup, H.; Rousselet, R.; Fantke, P. Evaluating the monetary values of greenhouse gases emissions in life cycle impact assessment. *Journal of Cleaner Production* **2019**, *209*, 538-549.

(63) Marten, A.L.; Newbold, S.C. Estimating the social cost of non-CO_2 GHG emissions: Methane and nitrous oxide. *Energy Policy* **2012**, *51*, 957-972.